Vehicle System Dynamics
2003, Vol. 39, No. 2, pp. 81–97

0042-3114/03/3902-081$16.00

Emergency Braking Control with an Observer-based Dynamic Tire/Road Friction Model and Wheel Angular Velocity Measurement

JINGANG YI[1], LUIS ALVAREZ[2], XAVIER CLAEYS[3]
AND ROBERTO HOROWITZ[4]

SUMMARY

A control scheme for emergency braking of vehicles is designed. The tire/road friction is described by a LuGre dynamic friction model. The control system output is the pressure in the master cylinder of the brake system. The controller utilizes estimated states for a feedback control law that achieves a near maximum deceleration. The state observer is designed using linear matrix inequality (LMI) techniques. The analysis shows that using the wheel angular speed information exclusively is not sufficient to rapidly estimate the velocity and relative velocity, due to the fact that the dynamical system is almost unobservable with this measurement as output. Findings are confirmed by simulation results that show that the estimated vehicle velocity and relative velocity converge slowly to their true values, even though the internal friction state and friction parameters converge quickly. The proposed control system has two main advantages when compared with an antilock braking system (ABS): (1) it produces a source of a priori information regarding safe spacing between vehicles that can be used to increase safety levels in the highway; and (2) it achieves a near optimal braking strategy with less chattering.

1. INTRODUCTION

In recent years, important research has been undertaken to investigate safety in both manual traffic and automated highway systems (AHS) when highway densities are significantly increased. One important issue that requires more careful analysis is the influence of the tire/road interaction on the braking capabilities of the vehicle and,

[1]Department of Mechanical Engineering, University of California, Berkeley, CA 94720-1740, USA. E-mail: jgyi@me.berkeley.edu
[2]Instituto de Ingeniería Universidad Nacional Autónoma de México, 04510 Coyoacán DF, México. E-mail: alvar@pumas.iingen.unam.mx
[3]Laboratoire d'Automatique de Grenoble, UMR CNRS 5528, ENSIEG-INPG, ST. Martin d'Hères, France. E-mail: claeys@lag.ensieg.inpg.fr
[4]Address correspondence to: Roberto Horowitz, Department of Mechanical Engineering, University of California, Berkeley, CA 94720-1740, USA. Tel.: +1-510-642-4675; Fax: +1-510-643-5599; E-mail: horowitz@me.berkeley.edu

therefore, on the overall highway safety. From the perspective of emergency braking, there are two main factors that determine this braking capacity: tire/road friction and available braking torque. Both are difficult to determine precisely due to modeling complexities and variations in the operating conditions.

There is a significant amount of research in tire/road friction modeling and estimation for individual vehicles. The model given in [1], known as the ''magic formula'', gives a good approximation to experimental results of the relationship between friction coefficient (μ) and longitudinal slip (λ), and is widely used in automotive research and industries. However, this model is complex and its parameters are generally difficult to calibrate and identify. In [2] and [3] identifiable pseudo-static parametric friction models, namely $\mu-\lambda$ curves, are presented. The parameters in these models lack a physical interpretation, but can be identified through on-line adaptation. A very nice property of the model given in [3] is the under-estimation of the friction coefficient under normal driving conditions, which guarantees vehicle safety.

In recent years, dynamic friction models, such as the one presented in [4], have been proposed to capture the friction mechanism. These models have been used successfully to identify and compensate the friction in mechanical systems. In [5], a first-order friction dynamic model, called the *LuGre* model, was first introduced to replicate the tire/road interface. This model was used in [6] to estimate the tire/road friction coefficient under different road conditions.

The goal of this paper is to design an emergency braking controller using a dynamic friction model under various tire/road conditions. In [7], the authors assumed that the friction internal state in the dynamic friction model and the vehicle longitudinal velocity information are measurable, which is not true in reality. In this paper, an observer will be constructed to estimate these state variables using only the measurable wheel angular velocity. The emergency braking controller then utilizes the estimated state variables and underestimation of longitudinal slip is achieved for vehicle stability. The difference of this paper from [6] is that we consider an adaptive emergency braking controller design using the observer-based dynamic friction model while in [6] an observer is constructed to detect the tire/road conditions under normal traction conditions.

The paper is divided in six sections. Section 2 describes the system dynamics. Section 3 discusses the control objectives for emergency braking maneuvers. Some tire/road characteristics are also discussed in this section. A compensator, which combines an adaptive controller with an observer, is presented in Section 4. A linear matrix inequality (LMI) technique is used to calculate the observer gains. Simulation results for this compensator are illustrated in Section 5, along with discussions of the limitations of schemes to estimate the longitudinal velocity based only on wheel angular velocity measurements. Finally, Section 6 contains concluding remarks and directions for future work.

2. SYSTEM DYNAMICS

In this paper only the longitudinal dynamics of the vehicle are considered. We assume that the four wheels of the vehicle apply the same braking force. For simplicity, we also assume that the road has no slope and that the weight of the vehicle is distributed evenly among the four wheels. A quarter vehicle model is used and we consider a modified lumped LuGre friction model as follows:

$$\begin{cases} \dot{z} = -v_r - \theta \frac{\sigma_0 |v_r|}{h(v_r)} z \\ J\dot{\omega} = -rF_x - u_\tau \\ m\dot{v} = 4F_x - F_r, \end{cases} \tag{1}$$

where z is the friction internal state, $v_r = v - r\omega$ is the relative velocity, $h(v_r) = \mu_c + (\mu_s - \mu_c)e^{-\left|\frac{v_r}{v_s}\right|^{1/2}}$, μ_s is the normalized static friction coefficient, μ_c is the normalized Coulomb friction, v_s is the Stribeck relative velocity, u_τ is the traction/braking torque, F_x the traction/braking force given by the tire/road contact, F_r the rolling resistance, m the vehicle mass, J the tire rotational inertia, and the parameter θ is used to model the effect of different tire/road Coulomb friction coefficients. The braking force F_x is given by:

$$F_x = F_n(\sigma_0 z + \sigma_1 \dot{z} - \sigma_2 v_r),$$

where σ_0 is the rubber longitudinal stiffness, σ_1 is the rubber longitudinal damping, and σ_2 is the viscous relative damping. F_x is a negative number in the case of braking and $F_n = mg/4$. According to [8], the rolling resistance can be modeled as:

$$F_r = \sigma_v mgv,$$

where σ_v is the rolling resistance coefficient and g is the gravity constant.

Defining the state variables as:

$$x_1 := \sigma_0 z, \qquad x_2 := v, \qquad x_3 := v_r = v - r\omega,$$

the system dynamics [Equation (1)] are rewritten as:

$$\dot{x}_1 = \sigma_0 \dot{z} = -\sigma_0 x_3 - \theta \sigma_0 f(x_3) x_1, \tag{2}$$

where $f(x_3) = \frac{x_3}{h(x_3)}$; here we use the fact that $x_3 = v_r = v - r\omega \geq 0$ during braking and

$$\dot{x}_2 = g[x_1 + \sigma_1(-x_3 - \theta f(x_3)x_1) - \sigma_2 x_3] - g\sigma_v x_2. \tag{3}$$

For the state variable x_3 we have:

$$\dot{x}_3 = \dot{v} - r\dot{\omega} = \alpha[x_1 + \sigma_1(-x_3 - \theta f(x_3)x_1) - \sigma_2 x_3] - g\sigma_v x_2 + \frac{r}{J} K_b P_b, \tag{4}$$

where $\alpha = g(1 + \frac{mr^2}{4J})$. In the above equation we use the formula $u_\tau = K_b P_b$, where K_b is the brake system gain and P_b the brake pressure, which is the controlled variable.

For most vehicles, we can measure the angular velocity of each wheel:

$$y = \omega = \frac{1}{r}(x_2 - x_3). \tag{5}$$

3. CONTROL DESIGN OBJECTIVES

The tire/road friction coefficient is defined by the ratio of traction/braking force (F_x) and the normal force (F_n) at the tire/road interface, that is:

$$\mu := \frac{F_x}{F_n}.$$

μ is a complex function of the vehicle longitudinal slip and other factors, such as tire and road conditions and vehicle velocity. The longitudinal slip λ is defined by:

$$\lambda := \begin{cases} \frac{v - r\omega}{v} & v \neq 0, \text{ braking,} \\ \frac{r\omega - v}{r\omega} & \omega \neq 0, \text{ traction.} \end{cases}$$

The pseudo-static relationship between μ and λ, usually called a pseudo-static curve, is shown schematically in Figure 1 for a given vehicle velocity and a set of

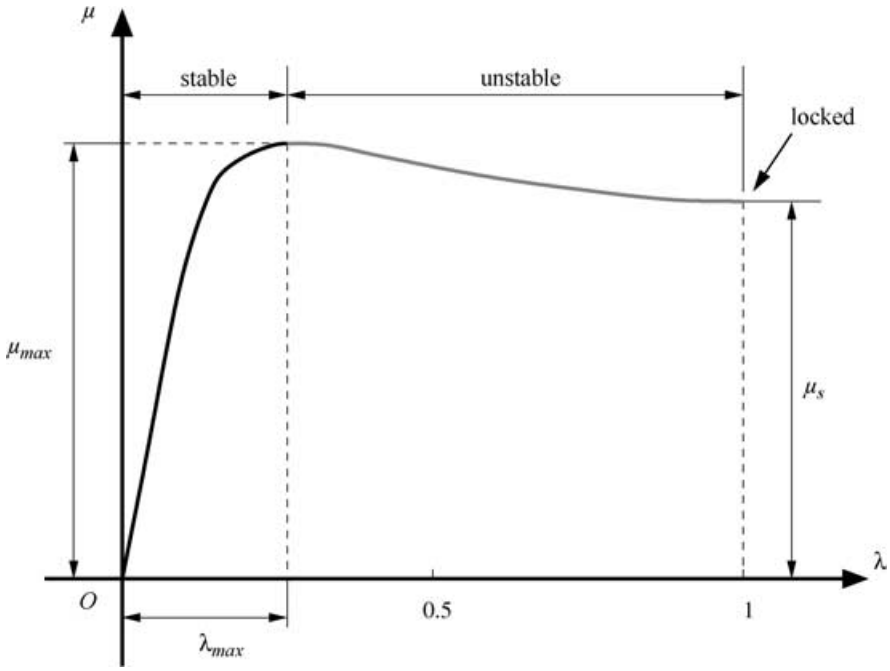

Fig. 1. A schematic of pseudo-static tire/road friction model (braking case).

tire/road conditions. As shown in the figure, the maximum friction coefficient, μ_{max} is achieved at a particular longitudinal slip, denoted as maximum slip $\lambda_{max} \in (0,\ 1)$. When the vehicle slip satisfies $\lambda \leq \lambda_{max}$, the vehicle motion is stable; otherwise, it is unstable. Moreover, the $\mu - \lambda$ curve varies under different tire/road conditions, vehicle normal forces, velocities, etc. Therefore, the maximum friction coefficient μ_{max} and maximum slip λ_{max} will change under varying environmental and vehicle conditions.

The objective of an emergency braking maneuver is to bring the vehicle to stop as quickly as possible. We need to design a braking controller that achieves a vehicle longitudinal slip close to λ_{max} while keeping the vehicle stable. In [9], a traction control was designed to force the slip to track λ_{max}, assuming that λ_{max} is known and fixed. In [10], a sliding mode controller and friction force observer achieve maximum friction force using an extremum seeking technique.

In this paper, we will use the LuGre dynamic tire/road friction model to estimate the maximum slip λ_{max} by means of an equivalent pseudo-static model. Assume that the vehicle velocity v is constant and the normal force is uniformly distributed on a rectangular tire/road contact patch. We can solve a distributed LuGre tire/road friction model and obtain following pseudo-static relationship between μ and λ, as in [7]:

$$\mu(\lambda, v, \theta) = \frac{h(v_r)}{\theta}\left[1 + 2\gamma\frac{h(v_r)}{\sigma_0\theta L|\eta|}\left(e^{-\frac{\sigma_0\theta L|\eta|}{2h(v_r)}} - 1\right)\right] + \sigma_2 v_r, \tag{6}$$

$$\eta = \frac{v_r}{r\omega} = \frac{\lambda}{1-\lambda}, \qquad \gamma = 1 - \frac{\sigma_1\theta|\eta|}{r\omega h(v_r)},$$

where L is the length of the tire/road contact patch.

Figure 2 shows that the equivalent pseudo-static $\mu - \lambda$ curve in Equation (6) fits the experimental data given in [11].

Remark 1 In [6], the friction curves are plotted when only the parameter θ is varied. The plots indicate that variation of parameter θ can capture different shapes of friction curves under various road conditions, which was reported in the literature. The analysis of the LuGre model shows that the most critical model parameter is σ_0, and θ tries in some way to capture the variations of this parameter. The variations of contact patch length L, due to change and shift of vehicle mass, can be absorbed through the friction model parameters, such as σ_0. In this paper, we only consider the variation of one parameter θ for simplicity.

Thus, assuming that v and θ are known, we can calculate the maximum slip λ_{max} by solving for it numerically from the equivalent pseudo-static model Equation (6):

$$\lambda_{max} = \arg\max_{\lambda}\{\mu(\eta, v, \theta)\}.$$

Note that the internal friction state z and the vehicle longitudinal velocity v are assumed not to be measurable, and the tire/road condition (θ) is unknown. It is

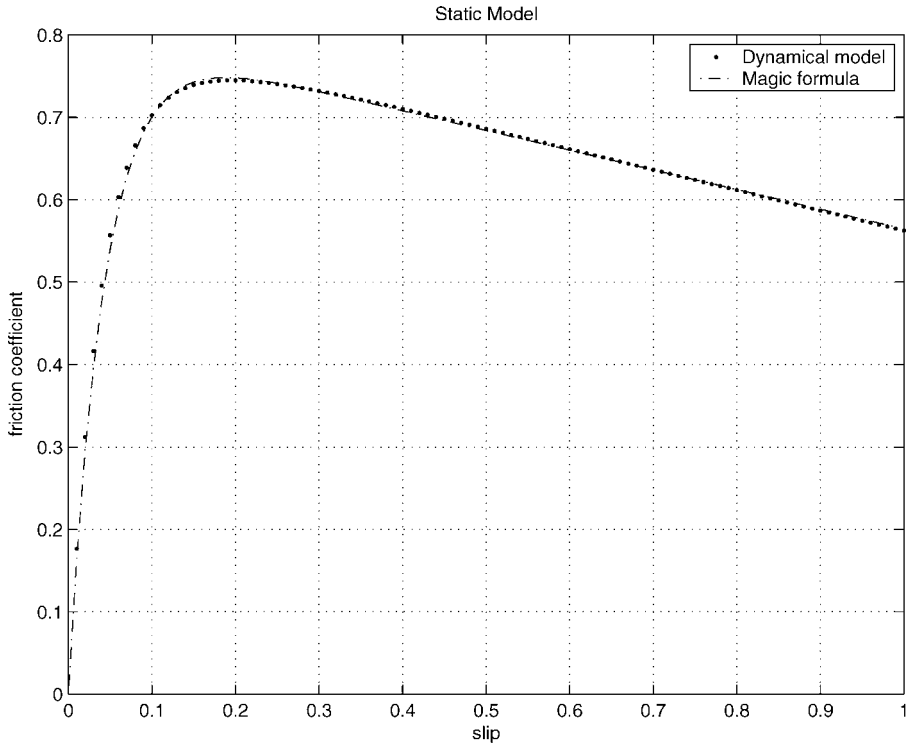

Fig. 2. Comparison of the dynamical model and the magic formula for a tire tested in braking with $v = 30\,mph$ and $\theta = 1$ in the model.

therefore difficult to obtain λ_{max} for current vehicle design. It is necessary to construct an observer to estimate these variables, so that near maximum deceleration can be achieved around $\hat{\lambda}_{max}$. $\hat{\lambda}_{max}$ can be determined from the estimated velocity ($\hat{v}$) and parameter ($\hat{\theta}$), that is:

$$\hat{\lambda}_{max} = \arg\max_{\hat{v},\lambda,\hat{\theta}} \{\hat{\mu}(\lambda, \hat{v}, \hat{\theta})\}, \tag{7}$$

if we can guarantee that $\hat{v} \to v$ and $\hat{\theta} \to \theta$.

Another important control objective is to achieve the underestimation of slip during an emergency braking maneuver, namely to ensure $\hat{\lambda}_{max}(t) \leq \lambda_{max}(t)$ for vehicle stability and to preserve the traffic safety.

In the following sections, we will describe an observer-based emergency braking controller design that satisfies these control objectives.

4. OBSERVER-BASED BRAKING CONTROLLER DESIGN

In this section, we formulate the design of a controller, based on the available angular velocity output. Arrange the system dynamics, Equations (2), (3), (4), and output measurements [Equation (5)] as follows:

$$\begin{cases} \dot{\mathbf{x}} = A\mathbf{x} + B_1\theta\psi(\mathbf{x}) + B_2 u \\ y = C\mathbf{x}, \end{cases} \tag{8}$$

where

$$\mathbf{x} = \begin{bmatrix} x_1 \\ x_2 \\ x_3 \end{bmatrix}, A = \begin{bmatrix} 0 & 0 & -\sigma_0 \\ g & -g\sigma_v & -g(\sigma_2+\sigma_1) \\ \alpha & -g\sigma_v & -\alpha(\sigma_2+\sigma_1) \end{bmatrix}, B_1 = \begin{bmatrix} -\sigma_0 \\ -g\sigma_1 \\ -\alpha\sigma_1 \end{bmatrix}, B_2 = \begin{bmatrix} 0 \\ 0 \\ \frac{r}{J}K_b \end{bmatrix},$$

$$C = \begin{bmatrix} 0 & \frac{1}{r} & -\frac{1}{r} \end{bmatrix}, \qquad \psi(\mathbf{x}) = x_1 f(x_3), \qquad u = P_b.$$

Since the internal state z, given by the LuGre model, and the vehicle longitudinal velocity are unavailable, we must design an observer to estimate these states. We therefore construct the following model-based nonlinear observer:

$$\dot{\hat{\mathbf{x}}} = A\hat{\mathbf{x}} + B_1\hat{\theta}\psi(\hat{\mathbf{x}}) + B_2 u + L(y - C\hat{\mathbf{x}}) + B_1\mathcal{G}, \tag{9}$$

where $\mathcal{G}$ is a tuning function to be determined subsequently.

The following assumptions are made for the system of Equation (8) and observer of Equation (9):

(i) (A, B_1) is controllable and (A, C) is observable;

(ii) $f(x_3)$ is non-negative and bounded and $f'(x_3)$ is bounded, that is,

$$0 \le f(x_3) \le f_{max} \le \rho_2 < \infty, \qquad |f'(x_3)| \le \rho_3 < \infty, \quad \forall \mathbf{x} \in \mathcal{D}_1 \subset \mathcal{R}. \tag{10}$$

(iii) The unknown parameter θ is bounded, that is:

$$0 < \theta \le \theta_{max}. \tag{11}$$

(iv) The map $w \mapsto \xi$ of the system

$$\begin{cases} \dot{\zeta} = (A - LC)\zeta + B_1 w \\ \xi = C\zeta \end{cases} \tag{12}$$

with $(A - LC)$ Hurwitz, is strictly passive; moreover, $\exists \rho_1 > 0$ a constant, and $\exists P = P^T > 0$ such that:

$$(A - LC)^T P + P(A - LC) + (\rho_1^2 + \rho_4)I < 0, \tag{13}$$

as well as

$$PB_1 = C^T, \tag{14}$$

where $\rho_4 = \frac{2\theta_{max}\rho_2}{r} > 0$.

Theorem 1 *Under assumptions* (*i*)–(*iv*) *there exists an adaptive emergency braking controller that achieves*

$$\hat{\lambda} \to \hat{\lambda}_{max}$$

asymptotically for the system of Equation (8) *using the measured angular velocity* ω, *where the estimated slip* $\hat{\lambda} := \frac{\hat{x}_3}{\hat{x}_2} = \frac{\hat{v}-r\hat{\omega}}{\hat{v}}$ *and* $\hat{\lambda}_{max} := \hat{\lambda}_{max}(\hat{v}_r, \hat{v})$ *is the longitudinal slip corresponding to the estimated maximum friction coefficient* $\hat{\mu}_{max}$ *in the pseudo-static relationship between* μ *and* λ, *given by Equation* (6).

Proof Define $\tilde{\mathbf{x}} := \mathbf{x} - \hat{\mathbf{x}}$, $\tilde{y} := y - \hat{y} = C\tilde{\mathbf{x}}$ and $\tilde{\theta} := \theta - \hat{\theta}$, then the error dynamics for the system is:

$$\dot{\tilde{\mathbf{x}}} = (A - LC)\tilde{\mathbf{x}} + B_1[\theta\psi(\mathbf{x}) - \hat{\theta}\psi(\hat{\mathbf{x}})] - B_1\mathcal{G}. \tag{15}$$

Define the dynamic surface $\tilde{s}$ as:

$$\tilde{s} := \hat{x}_3 - \hat{\lambda}_{max}\hat{x}_2,$$

and differentiate $\tilde{s}$:

$$\begin{aligned}
\dot{\tilde{s}} &= \dot{\hat{x}}_3 - \dot{\hat{x}}_2\hat{\lambda}_{max} - \dot{\hat{\lambda}}_{max}\hat{x}_2 \\
&= \frac{r}{J}K_bP_b - \sigma_1(\alpha - g\hat{\lambda}_{max})f(\hat{x}_3)\hat{\theta} + \\
&\quad + \{(\alpha - g\hat{\lambda}_{max})[\hat{x}_1 - (\sigma_2 + \sigma_1)\hat{x}_3 - (1 - \hat{\lambda}_{max})g\sigma_v\hat{x}_2] + \\
&\quad + (l_3 - l_2\hat{\lambda}_{max})\tilde{y}\} - \sigma_1(\alpha - g\hat{\lambda}_{max})\mathcal{G} - \dot{\hat{\lambda}}_{max}\hat{x}_2 \\
&= dK_bP_b + \beta_1(\hat{\mathbf{x}})\hat{\theta} + \beta_2(\hat{\mathbf{x}}) + \beta_3(\hat{\mathbf{x}})\mathcal{G},
\end{aligned} \tag{16}$$

where $d = \frac{r}{J}$,

$$\begin{aligned}
\beta_1(\hat{\mathbf{x}}) &= -\sigma_1(\alpha - g\hat{\lambda}_{max})f(\hat{x}_3)\hat{x}_1, \\
\beta_2(\hat{\mathbf{x}}) &= (\alpha - g\hat{\lambda}_{max})[\hat{x}_1 - (\sigma_2 + \sigma_1)\hat{x}_3] + \\
&\quad + (l_3 - l_2\hat{\lambda}_{max})\tilde{y} - \dot{\hat{\lambda}}_{max}\hat{x}_2 - (1 - \hat{\lambda}_{max})g\sigma_v\hat{x}_2, \\
\beta_3(\hat{\mathbf{x}}) &= -\sigma_1(\alpha - g\hat{\lambda}_{max}),
\end{aligned}$$

and l_2, l_3 are the second and third elements of the gain vector $L \in \mathcal{R}^3$.

Consider the following Lyapunov function candidate:

$$V = \frac{1}{2}\tilde{s}^2 + \frac{1}{2\gamma}\tilde{\theta}^2 + \tilde{\mathbf{x}}^T P \tilde{\mathbf{x}},$$

where $\gamma > 0$. Then

$$\begin{aligned}\dot{V} &= \dot{\tilde{\mathbf{x}}}^T P\tilde{\mathbf{x}} + \tilde{\mathbf{x}}^T P\dot{\tilde{\mathbf{x}}} + \tilde{s}\dot{\tilde{s}} + \frac{1}{\gamma}\tilde{\theta}\dot{\tilde{\theta}} \\ &= \tilde{\mathbf{x}}^T[(A-LC)^T P + P(A-LC)]\tilde{\mathbf{x}} + 2\tilde{\mathbf{x}}^T PB_1[\theta\psi(\mathbf{x}) - \hat{\theta}\psi(\hat{\mathbf{x}})] + \\ &\quad + \frac{1}{\gamma}\tilde{\theta}\dot{\tilde{\theta}} + \tilde{s}\dot{\tilde{s}} - 2\tilde{\mathbf{x}}^T PB_1\mathcal{G}.\end{aligned}$$

Notice that

$$\theta\psi(\mathbf{x}) - \hat{\theta}\psi(\hat{\mathbf{x}}) = \tilde{\theta}\psi(\hat{\mathbf{x}}) + \theta[\psi(\mathbf{x}) - \psi(\hat{\mathbf{x}})],$$

and use fact in Equation (14) to obtain:

$$\begin{aligned}\dot{V} &= \tilde{\mathbf{x}}^T[(A-LC)^T P + P(A-LC)]\tilde{\mathbf{x}} + 2\tilde{y}\tilde{\theta}\psi(\hat{\mathbf{x}}) + \\ &\quad + 2\tilde{\mathbf{x}}^T PB_1\theta[\psi(\mathbf{x}) - \psi(\hat{\mathbf{x}})] + \frac{1}{\gamma}\tilde{\theta}\dot{\tilde{\theta}} + \\ &\quad + \tilde{s}[dK_b P_b + \beta_1(\hat{\mathbf{x}})\hat{\theta} + \beta_2(\hat{\mathbf{x}}) + \beta_3(\hat{\mathbf{x}})\mathcal{G}] - 2\tilde{\mathbf{x}}^T PB_1\mathcal{G}. \qquad (17)\end{aligned}$$

Let the control input be:

$$u = P_b = \frac{1}{dK_b}[-\beta_1(\hat{\mathbf{x}})\hat{\theta} - \beta_2(\hat{\mathbf{x}}) - \beta_3(\hat{\mathbf{x}})\mathcal{G} - \xi\tilde{s}],$$

where $\zeta > 0$, then Equation (16) becomes:

$$\dot{\tilde{s}} = -\xi\tilde{s}. \qquad (18)$$

Using Equations (14) and (18) and letting:

$$\dot{\hat{\theta}} = 2\gamma\tilde{y}\psi(\hat{\mathbf{x}}), \qquad (19)$$

we obtain from Equation (17):

$$\begin{aligned}\dot{V} &= \tilde{\mathbf{x}}^T[(A-LC)^T P + P(A-LC)]\tilde{\mathbf{x}} + \\ &\quad + 2\tilde{\mathbf{x}}^T PB_1\theta[\psi(\mathbf{x}) - \psi(\hat{\mathbf{x}})] - \xi\tilde{s}^2 - 2\tilde{y}\mathcal{G}.\end{aligned}$$

Note that

$$\psi(\mathbf{x}) - \psi(\hat{\mathbf{x}}) = x_1 f(x_3) - \hat{x}_1 f(\hat{x}_3) = f(x_3)\tilde{x}_1 + \hat{x}_1 f'(x_3^*)(x_3 - \hat{x}_3), \qquad (20)$$

where x_3^* is a value between x_3 and $\hat{x}_3$ derived by applying the Mean Value Theorem to the smooth function $f(x) = \frac{x}{h(x)}$. Moreover, by Equations (10), (11) and (20):

$$\begin{aligned}
\dot{V} &\le \tilde{\mathbf{x}}^T[(A-LC)^TP + P(A-LC)]\tilde{\mathbf{x}} + 2\tilde{\mathbf{x}}^T C^T \theta_{max}\rho_2\tilde{x}_1 + \\
&\quad + 2\rho_3\theta_{max}|\tilde{y}||\hat{x}_1||\tilde{x}_3| - \xi\tilde{s}^2 - 2\tilde{y}\mathcal{G} \\
&= \tilde{\mathbf{x}}^T[(A-LC)^TP + P(A-LC)]\tilde{\mathbf{x}} + \frac{1}{r}\theta_{max}\rho_2(2\tilde{x}_1\tilde{x}_2 - 2\tilde{x}_1\tilde{x}_3) + \\
&\quad + 2\rho_3\theta_{max}|\tilde{y}||\hat{x}_1||\tilde{x}_3| - \xi\tilde{s}^2 - 2\tilde{y}\mathcal{G} \\
&\le \tilde{\mathbf{x}}^T[(A-LC)^TP + P(A-LC)]\tilde{\mathbf{x}} + \rho_4\left(\tilde{x}_1^2 + \frac{1}{2}\tilde{x}_2^2 + \frac{1}{2}\tilde{x}_3^2\right) - \\
&\quad - \frac{\rho_4}{2}\left(|\tilde{x}_3| - \frac{\rho_3 r}{\rho_2}|\tilde{y}\hat{x}_1|\right)^2 + \frac{\rho_4}{2}\tilde{x}_3^2 + \frac{\rho_4}{2}\left(\frac{\rho_3 r}{\rho_2}\right)^2\hat{x}_1^2\tilde{y}^2 - \xi\tilde{s}^2 - 2\tilde{y}\mathcal{G} \\
&\le \tilde{\mathbf{x}}^T\ [(A-LC)^TP + P(A-LC) + \rho_4 I]\tilde{\mathbf{x}} - \xi\tilde{s}^2 - \\
&\quad - \frac{\rho_4}{2}\left(|\tilde{x}_3| - \frac{\rho_3 r}{\rho_2}|\tilde{y}\hat{x}_1|\right)^2 + \tilde{y}\left[\frac{\rho_4}{2}\left(\frac{\rho_3 r}{\rho_2}\right)^2\hat{x}_1^2\tilde{y} - 2\mathcal{G}\right] \\
&\le -\rho_1^2\|\tilde{\mathbf{x}}\|^2 - \xi\tilde{s}^2 - \frac{\rho_4}{2}\left(|\tilde{x}_3| - \frac{\rho_3 r}{\rho_2}|\tilde{y}\hat{x}_1|\right)^2 + \tilde{y}\left[\frac{\rho_4}{2}\left(\frac{\rho_3 r}{\rho_2}\right)^2\hat{x}_1^2\tilde{y} - 2\mathcal{G}\right].
\end{aligned}$$

If we choose $\mathcal{G}$ such that:

$$\mathcal{G} = \frac{\rho_4}{4}\left(\frac{\rho_3 r}{\rho_2}\right)^2\hat{x}_1^2\tilde{y}, \tag{21}$$

then

$$\dot{V} \le -\rho_1^2\|\tilde{\mathbf{x}}\|^2 - \xi\tilde{s}^2 - \frac{\rho_4}{2}\left(|\tilde{x}_3| - \frac{\rho_3 r}{\rho_2}|\tilde{y}\hat{x}_1|\right)^2 \le 0.$$

Using Barbalat's Lemma, we can conclude that

$$\tilde{s} \to 0, \qquad \tilde{\mathbf{x}} \to 0, \quad \text{as } t \to \infty.$$

Thus, by definition of $\tilde{s}$ and λ we have

$$\hat{\lambda} \to \hat{\lambda}_{max}, \quad \text{as } t \to \infty.$$

Remark 2 To compute the controlled input P_b we need to know $\hat{\lambda}_{max}$ and $\dot{\hat{\lambda}}_{max}$. We use Equation (7) to calculate the estimated maximum slip $\hat{\lambda}_{max}$ under current estimated vehicle velocity and tire/road conditions. $\dot{\hat{\lambda}}_{max}$ is then calculated numerically.

Remark 3 The adaptive nonlinear observer structure presented in this paper is similar to the scheme presented in [12], although the results in [12] require an

additional Lipschitz assumption on the function $\psi(x)$, and the condition of Equation (14) is replaced by $B_1^T P C^{\perp} = 0$, where $C^{\perp}$ is the projection onto null(C).

Remark 4 The tuning function $\mathcal{G}$ given by Equation (21) is a linear function of $\tilde{y}$ and appears both in the observer and the control input. Compared with the tuning function in [6], Equation (21) does not require switching in the control input, and therefore produces a smoother control.

Remark 5 Assumptions (i) through (iv) must be satisfied by the system dynamics described by Equation (8) for the theorem to hold:

(i) Regarding assumption (i), we can calculate the observability matrix:

$$\mathcal{O} = \begin{bmatrix} 0 & \frac{1}{r} & -\frac{1}{r} \\ \frac{g-\alpha}{r} & 0 & \frac{a}{r} \\ \frac{\alpha a}{r} & -\frac{g\sigma_v a}{r} & \frac{(g-\alpha)[\alpha(\sigma_2+\sigma_1)^2+\sigma_0]}{r} \end{bmatrix},$$

where $a = (\sigma_2 + \sigma_1)(\alpha - g)$, thus $rank(\mathcal{O}) = 3$, and (A,C) is an observable pair. Similarly, the controllability matrix $\mathcal{C} = \begin{bmatrix} B_1 & AB_1 & A^2B_1 \end{bmatrix}$ satisfies $rank(\mathcal{C}) = 3$. Hence, assumption (i) always holds;

(ii) To see that assumption (ii) is always satisfied, we have:

$$0 \le f(x_3) = \frac{x_3}{h(x_3)} \le \frac{x_3}{\mu_c} \le \frac{\lambda_{max} v_{max}}{\mu_c} = \rho_2,$$

and

$$|f'(x_3)| \le \frac{1}{\mu_c}\left\{1 + \left(\frac{\mu_s}{\mu_c} - 1\right)\left[1 + \frac{1}{2}\left(\frac{v_{max}}{v_s}\right)^{1/2}\right]\right\} = \rho_3.$$

(iii) Assumption (iv) is satisfied by construction. As for (iv), we have to pick an observer gain L and a positive symmetric matrix P such that following optimization problem is feasible:

$$\begin{cases} \max \quad \rho_1 \\ \text{s.t.:} \quad (A - LC)^T P + P(A - LC) + \rho_1^2 I + \rho_4 I < 0 \\ \qquad PB_1 = C^T, \quad P = P^T > 0 \quad \text{and} \quad \rho_1 > 0 \end{cases}$$

This can be calculated by linear matrix inequality (LMI) algorithms, such as those presented in [13].

5. SIMULATION RESULTS AND DISCUSSIONS

In the following simulation example we use the parameters from the LeSabre cars used by the California PATH program. These parameters are: $M = 1701.0\,Kg$,

$\sigma_v = 0.005\,N \cdot s^2/m^2$, $J = 2.603\,Kg \cdot m^2$, $r = 0.323\,m$. We also take the road LuGre friction parameter in Equation (1) to be $\theta = 1$ and the braking gain $K_b = 0.9$. The nominal values of the parameters in the dynamic LuGre friction model are the same as those in [7].

We simulate an emergency braking maneuver with a vehicle initial velocity of $v = 30\,m/s$ and the designed observer-based controller. The initial condition for the observer dynamics is $\hat{\mathbf{x}}(0) = [0\ 29.5\ 0]^T$ and the true state is $\mathbf{x}(0) = [0\ 30\ 0.5]^T$; namely we use the measurement $r\omega(= 29.5\,m/s)$ as the initial condition for $\hat{v}$. Figure 3 shows the time responses of the real state vector $\mathbf{x}$ and estimated state vector $\hat{\mathbf{x}}$, while

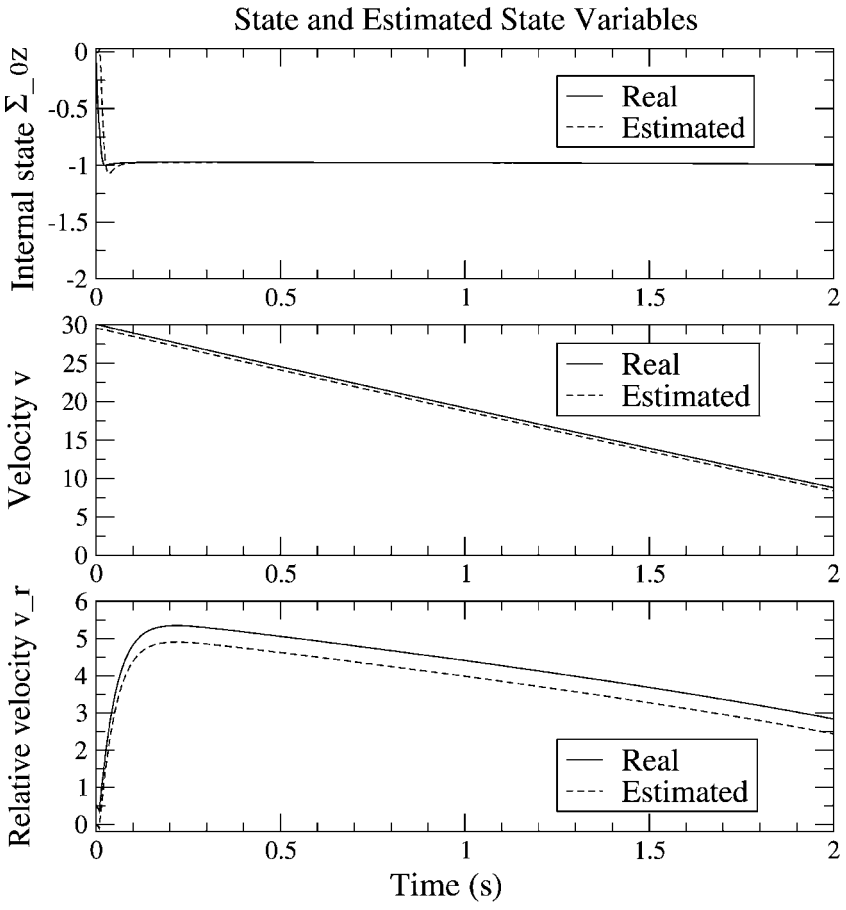

Fig. 3. Estimated and real state variables.

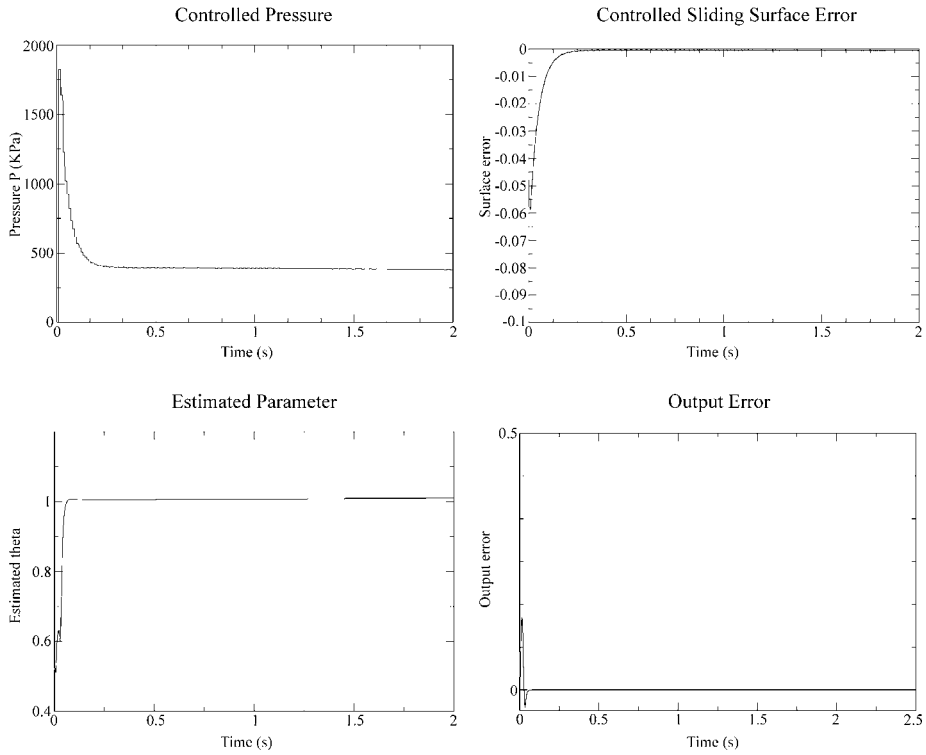

Fig. 4. (a) Controlled braking pressure P. (b) Sliding surface $\tilde{s}$. (c) Estimated friction parameter $\hat{\theta}$. (d) Measurement error $\tilde{y}$ (*rad/s*).

Figure 4(c) shows the time response of the estimated friction parameter $\hat{\theta}$. Figure 4(a) shows the time response of the controlled pressure P while Figure 4(b) shows the controlled sliding surface $\tilde{s}$. Figure 4(d) illustrates the difference, $\tilde{y}$, between the measurement y and output of observer $\hat{y}$. From these figures we can see that the estimated state $\hat{z}$ and parameter $\hat{\theta}$ converge to their respective true values quickly, and that the controlled input (pressure P) remains within its feasible domain, enabling the vehicle to come to a quick halt (decelerating at around $10\,m/s^2$). This example verifies the results of the previous section. However, the simulation results also reveal that the estimated states $\hat{v}$ and $\hat{v}_r$ do not converge to their true states during the braking process, remaining within a constant offset, even though the vehicle achieved its maximum estimated deceleration level, which is based on estimated states, as shown by Figure 4(b).

In what follows we present a formal explanation of the above simulation results.

From the state error dynamics of Equation (15) we find that

$$\dot{\tilde{\mathbf{y}}} = -\frac{1}{r}[l_2 - l_3 + \sigma_1(g-\alpha)\mathbf{g}]\tilde{\mathbf{y}} + f_1(\tilde{\mathbf{x}}), \tag{22}$$

where $f_1(\tilde{\mathbf{x}}) = (g-\alpha)[(1-\sigma_1\theta f(x_3)]\tilde{x}_1 - \sigma_v\tilde{x}_2 - (\sigma_1+\sigma_2)\tilde{x}_3 - \sigma_1[\theta f(x_3) - \hat{\theta}f(\hat{x}_3)]\hat{x}_1$ and $\mathbf{g} = \frac{\rho_4}{4}(\frac{\rho_3 r}{\rho_2})^2\hat{x}_1^2$. In our example, we chose a relatively large value for the gain L with $l_2 > l_3$ ($L = [-400 \ -60 \ -500]^T$). As a consequence, $\tilde{y} \to 0$ quickly. Similarly, we can also assume that $\tilde{\theta} \to 0$ quickly, due to our choice of a high adaptation gain ($\gamma = 200$) and the presence of persistence of excitation, which we observed in the numerical example. The analysis for absence of persistence of excitation is in progress.

Using the approximation $\tilde{y} \approx 0$ and $\tilde{\theta} \approx 0$, we now analyze the dynamics of the state errors of Equation (15) and obtain

$$\dot{\tilde{\mathbf{x}}} = \bar{A}(x_3)\tilde{\mathbf{x}}, \tag{23}$$

where

$$\bar{A}(x_3) = \begin{bmatrix} -\sigma_0\theta f(x_3) & 0 & 0 \\ g[1-\sigma_1\theta f(x_3)] & -g\sigma_v & -g\sigma_2 \\ \alpha[1-\sigma_1\theta f(x_3)] & -g\sigma_v & -\alpha\sigma_2 \end{bmatrix}.$$

Notice that $\sigma_0 = 280$, $\hat{\theta} \approx 1$ and $\frac{v}{\mu_c} \geq f(x_3) > \frac{v_r}{\mu_s}$. We can therefore conclude that $\tilde{x}_1 \to 0$ quickly with a decay rate of around $\sigma_0\theta f(x_3)$ during the beginning of the braking process, due to the fact that v_r is large. This explains why the estimated state $\hat{x}_1$ converges quickly to the real state x_1. In the case of the state estimates $\hat{x}_2$ and $\hat{x}_3$, from Equation (23) we find that the eigenvalues of matrix $\bar{A}(x_3)$ associated with these two states are:

$$s_{2,3} = \frac{-(g\sigma_v + \alpha\sigma_2) \pm \sqrt{(g\sigma_v)^2 + (\alpha\sigma_2)^2 + 4g^2\sigma_v\sigma_2}}{2}.$$

Since σ_v and σ_2 are very small,

$$-1 \ll s_{2,3} < 0, \quad \forall t \geq 0.$$

The rate of decay for $\tilde{x}_2$ and $\tilde{x}_3$ is small and the eigenvector associated with s_2 is around $w_2 \approx [0\,1\,1]^T$.

Figure 5 shows a sketch of the trajectory portrait of the approximate nonlinear system in Equation (23). For any initial condition $P_0 = (\tilde{x}_1(0), \tilde{x}_2(0), \tilde{x}_3(0)) \in \mathcal{R}^3$, the flow trajectory will quickly approach the $\tilde{x}_2 \times \tilde{x}_3$ plane because of the rapid convergence of $\tilde{x}_1$ (s_1 is large). Moreover, the trajectory will converge to w_2 on the $\tilde{x}_2 \times \tilde{x}_3$ plane if $\tilde{x}_2(0) > 0$ and $\tilde{x}_3(0) > 0$, as shown in Figure 5. Thus, if we pick

$$\tilde{x}_2(0) \geq 0, \qquad \tilde{x}_3(0) \geq 0, \tag{24}$$

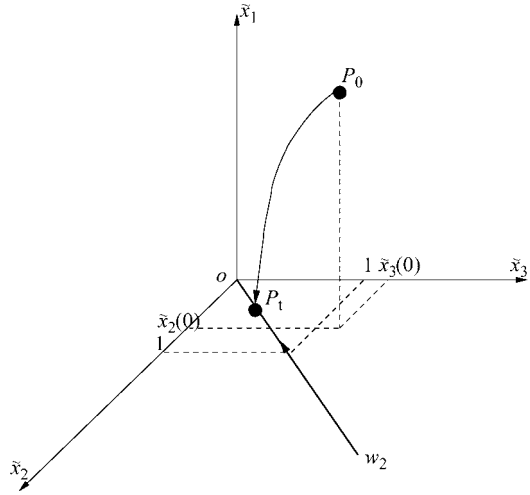

Fig. 5. A schematic trajectory plot for nonlinear system $\dot{\tilde{\mathbf{x}}} = \bar{A}(x_3)\tilde{\mathbf{x}}$.

then

$$\max\{\tilde{x}_2(0), \tilde{x}_3(0)\} \geq \tilde{x}_2(t) \approx \tilde{x}_3(t) \geq 0, \quad \forall\, t \geq t_0.$$

where t_0 is fairly small and depends on the convergence rate and initial conditions of $\tilde{x}_1(t)$.

When the angular velocity is the only measurement available to the control system and a state observer is designed, the angular velocity estimation error can be expressed as:

$$\tilde{\omega} = \omega - \hat{\omega} = \frac{1}{r}(x_2 - x_3) - \frac{1}{r}(\hat{x}_2 - \hat{x}_3) = \frac{1}{r}(\tilde{x}_2 - \tilde{x}_3). \tag{25}$$

It should be noticed that $\tilde{\omega} = 0$ does not imply that $\tilde{x}_2 = \tilde{x}_3 = 0$ but that $\tilde{x}_2 = \tilde{x}_3$. Vector w_2 in Figure 5 belongs to the surface where $\tilde{\omega} = 0$. It is important to remark that this limitation obeys the relation between x_2 and x_3 and is not dependent on the dynamic friction model or observer structure that was used in this paper.

Note that, by Theorem 1, we obtained $\hat{\lambda} \to \hat{\lambda}_{max}$ and $\lambda \to \lambda_{max}$, due to the fact $\hat{\mathbf{x}} \to \mathbf{x}$. However, since the states $\hat{x}_3$ and $\hat{x}_2$ converge slowly, there will be some error between λ and $\hat{\lambda}$. This error can be estimated as follows:

$$\begin{aligned} 0 < \lambda(t) - \hat{\lambda}(t) &= \frac{x_3}{x_2} - \frac{\hat{x}_3}{\hat{x}_2} = \frac{x_2\tilde{x}_3 - x_3\tilde{x}_2}{x_2\hat{x}_2} \\ &\approx \frac{(x_2 - x_3)\tilde{x}_2}{x_2\hat{x}_2} = \left(1 - \frac{x_3}{x_2}\right)\frac{\tilde{x}_2}{\hat{x}_2} \qquad (26) \\ &\leq (1 - \lambda(t))\,\frac{\lambda(0)x_2(0)}{\hat{x}_2(t)}, \quad \forall t \geq t_0. \qquad (27) \end{aligned}$$

Note that in general $\lambda(0) \leq 3\%$ during normal driving conditions before braking. As a consequence, the slip estimate error is small. Similarly, it can be shown that $\lambda_{max} - \hat{\lambda}_{max}$ will also be small after the state $\tilde{x}_1 \to 0$. Therefore, the proposed control system will achieve a near maximum deceleration level, in spite of the fact that state estimation errors $\tilde{x}_2$ and $\tilde{x}_3$ converge slowly.

Remark 6 It should be noticed that by the controller design, we can always guarantee the underestimation of longitudinal slip $\lambda(t)$ as shown in Equation (27). This is a very important property, which helps to preserve the vehicle safety and stability on the highway, since the safe inter-vehicle space depends on the estimation of maximum acceleration and deceleration.

6. CONCLUSIONS

In this paper we first discussed emergency braking control under unknown tire/road conditions and system states, based on a dynamical friction model and the assumption that the only available measurable signal for the controller is the wheel angular velocity. The braking pressure controller is determined based on the estimation of system state variables and the unknown friction parameter. The simulation results show that the vehicle can be stopped quickly with near maximum deceleration by applying this controller. The asymptotic convergence of the estimated states and parameter estimates has been proven. Moreover, it was also shown that the friction properties can be estimated and near maximum deceleration achieved, in spite of the slow convergence rate of the vehicle velocity and wheel relative velocity error estimates. Fortunately, both automated highway systems (AHS) and manual traffic applications rely on various other measurements to guarantee safety (e.g., radar sensors and human perception). Thus, the control system does not need an accurate estimate of the vehicle velocity. Simulation tests conducted so far suggest that the proposed control scheme, based on an observed dynamic friction model, achieves near maximum deceleration in a faster and more stable manner than previous static approaches.

ACKNOWLEDGEMENTS

The authors would like to thank Professor Carlos Canudas de Wit at Laboratoire d'Automatique de Grenoble, ENSIEG-INPG, France for various discussions and helpful suggestions. The authors also thank the anonymous reviewers for their suggestions and comments. The first, second and fourth authors acknowledge the support of California PATH program under MOU 373. The third author also thanks

for the support from the Renault Research Division in France during his visit at the Department of Mechanical Engineering, University of California at Berkeley, USA.

REFERENCES

1. Bakker, E., Nyborg, L. and Pacejka, H.B.: Tyre Modelling for Use in Vehicle Dynamic Studies. *SAE Paper* No. 870421, 1987.
2. Kiencke, U.: Realtime Estimation of Adhesion Characteristic Between Tyres and Road. In: *Proceedings of the IFAC World Congress*, Vol. 1, 1993.
3. Yi, J., Alvarez, L. and Horowitz, R.: Adaptive Emergency Braking Control with Underestimation of Friction Coefficient. In: *IEEE Transactions on Control Systems Technology* 10(3) (2002), pp. 381–392.
4. Canudas de Wit, C., Olsson, H., Åström, K.J. and Lischinsky, P.: A New Model for Control of Systems with Friction. *IEEE Transactions on Automatic Control* 40(3) (1995), pp. 419–425.
5. Canudas de Wit, C. and Tsiotras, P.: Dynamic Tire Friction Models for Vehicle Traction Control. In: *Proceedings of* 38*th IEEE Conference of Decision and Control*, Phoenix, AZ, 1999.
6. Canudas de Wit, C. and Horowitz, R.: Observers for Tire/Road Contact Friction Using Only Wheel Angular Velocity Information. In: *Proceedings of* 38*th IEEE Conference of Decision and Control*, Phoenix, AZ, 1999.
7. Yi, J., Alvarez, L., Horowitz, R. and Canudas de Wit, C.: Adaptive Emergency Braking Control in Automated Highway System Using Dynamic Tire/Road Friction Model. In: *Proceedings of* 39*th IEEE Conference of Decision and Control*, Sydney, Australia, 2000, pp. 456–461.
8. Wong, J.Y.: *Theory of Ground Vehicles*. Wiley, New York, 2nd ed., 1993.
9. Tan, H.S. and Tomizuka, M.: An Adaptive Sliding Mode Vehicle Traction Controller Design. In: *The American Control Conference*, San Diego, California, 1990, pp. 1156–1161.
10. Drakunov, S., Ozguner, U., Dix, P. and Ashrafi, B.: ABS Control Using Optimum Search via Sliding Modes. *IEEE Transactions on Control Systems Technology* 3(1) (1995), pp. 79–85.
11. Schuring, D.J.: Tire Parameter Determination. *DOT* HS-802 089, Calspan Corporation, 1976.
12. Cho, Y.M. and Rajamani, R.: A Systematic Approach to Adaptive Observer Synthesis for Nonlinear Systems. *IEEE Transactions on Automatic Control* 42(4) (1997), pp. 534–537.
13. El Ghaoui, L., Nikoukhah, R. and Delebecque, F.: LMITOOL: A Package for LMI Optimization. In: *Proceedings of* 34*th IEEE Conference of Decision and Control*, New Orleans, LA, 1995.